Transactions of the Materials Research Society of Japan 29[6] 2559-2562 (2004)

High Resolution TEM Study of $Li_2NiMn_3O_8$ and Li_2MnNiO_4 for Advanced Lithium Batteries

N. Nakayama, T. Mizota, T. Ohzuku* and Y. Ueda**

Faculty of Engineering, Yamaguchi University, Ube 755-8611, Japan
*Graduate School of Engineering, Osaka City University, Osaka 558-8585, Japan
**ISSP, the University of Tokyo, Kashiwa 277-8581, Japan
Fax: 81-836-85-9601, e-mail: nakayamn@yamaguchi-u.ac.jp

The cationic ordering in two new lithium insertion materials for advanced batteries, $Li_2NiMn_3O_8$ and Li_2MnNiO_4, has been investigated by high-resolution TEM. Spinel-type $Li_2NiMn_3O_8$, showing high operating voltage at 4.7 V of Li/ $Li_2NiMn_3O_8$ cell and very flat charge-discharge curve, has an 1:3 ordered arrangement of Ni and Mn in the spinel B-sites with $P4_332$ or $P4_132$ symmetry. The well-ordered cationic arrangement is crucial for the cell performance and it is obtained by annealing samples below 700°C. Li_2MnNiO_4, showing high rechargeable capacity more than 200 mAh/g, has a layered α-$NaFeO_2$-type fundamental lattice. Electron diffraction patterns show extra spots indicating a $\sqrt{3} \times \sqrt{3}$ superlattice in the basal triangular lattice and a layer stacking in a monoclinic C2/m symmetry. However, extra spots accompany the diffuse streak indicating stacking faults. Lattice images revealed that the cationic ordering is short-ranged in the basal plane and the stacking is disordered. The origins of the $\sqrt{3} \times \sqrt{3}$ superlattice are discussed.

Key words: lithium-ion battery, positive-electrode material, cationic ordering, lattice image, electron diffraction

1. INTRODUCTION

$LiCoO_2$ is widely used for positive-electrode materials in rechargeable lithium-ion batteries. Because cobalt is more expensive than other transition metals, Mn and Ni, commonly used in the batteries, the alternative materials have been investigated extensively for the last two decades. The promising candidates were $LiNiO_2$ [1,2] with a layered α-$NaFeO_2$-type structure isostructural to $LiCoO_2$ and $LiMn_2O_4$ [3] with a spinel-type structure. The drawback of these two materials compared with $LiCoO_2$ has been overcome to a certain extent by doping the third metallic elements [4]. Recently, Ohzuku et al. have developed new positive-electrode materials in the quaternary Li-Mn-Ni-O system. The one of them is $Li_2NiMn_3O_8$ with spinel-type structure [5-8]. Li/$Li_2NiMn_3O_8$ cell shows high operating voltage of 4.7V with good flatness of charge-discharge curve and with the enough discharge capacities exceeding 130 mAh/g. Another one is Li_2MnNiO_4 with α-$NaFeO_2$ type structure [9-11]. The Li/Li_2MnNiO_4 cell shows discharge capacities more than 200mAh/g with small polarization. Li_2MnNiO_4 may be an alternative positive-electrode material to $LiCoO_2$.

The details of crystal structures of these two new positive-electrode materials still remain uncertain, particularly on the cationic distributions because the x-ray atomic scattering factors of Ni and Mn are close together. The reported variation of cell properties depending on the sample preparation method and conditions suggests some difference in the cationic distribution from sample to sample. In this report, we will present transmission electron microscopy (TEM) study on the cationic arrangement in the above two new positive-electrode materials.

2. EXPERIMENTAL

The battery active samples of $Li_2NiMn_3O_8$ and Li_2MnNiO_4 were prepared by heating the mixtures of lithium hydroxide and nickel-manganese mixed hydroxide (from Tanaka Chemical Co. Ltd.) The details of the sample preparations have been reported elsewhere[5-11]. To clarify the phase relation in the quaternary Li-Ni-Mn-O system, samples were prepared by heating the mixtures of lithium hydroxide, nickel hydroxide and manganese carbonate. Samples were identified and characterized by power x-ray diffraction method. For TEM observations, samples were dispersed in ethanol by applying the ultrasonic wave and were collected on a holly micro grid supported on a copper grid mesh. A field emission type TEM (JEOL JEM2010F) operated at 200kV was used for the observations.

3. RESULTS and DISCUSSION

3.1 Phase relations in the Li-Mn-Ni-O system

More than 50 samples with different compositions have been prepared by the direct reactions of lithium hydroxide, nickel hydroxide and manganese carbonates to investigate the phase relations of Li-Mn-Ni-O quaternary oxides. Figures 1(a) and (b) summarize the obtained products on the pseudo-ternary diagram for samples annealed in air at 700 and 850°C, respectively.

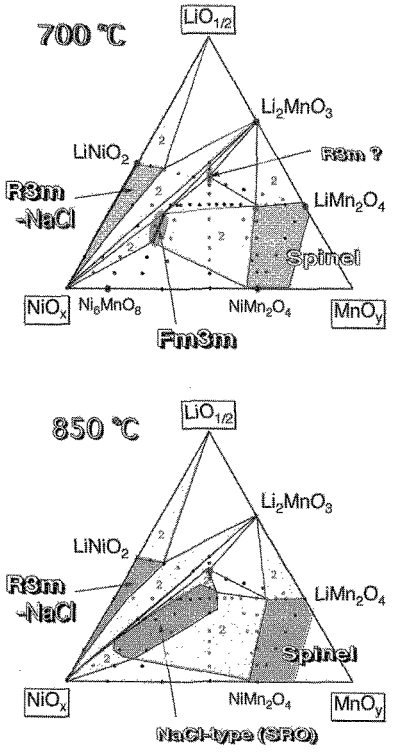

Fig.1 The products-composition diagrams in the quaternary Li-Ni-Mn-O phases prepared by the direct reaction of $LiOH{\cdot}H_2O$, $Ni(OH)_2$, and $MnCO_3$. They are heated at 700 and 850°C for 2 days and quenched to room temperature.

All the samples were air quenched into liquid nitrogen from the annealing temperature. Under the above heating conditions, spinel-type $(Li,Mn,Ni)_3O_4$ solid solutions and NaCl-type NiO-$LiNiO_2$ solid solutions are obtained in fairly wide compositional ranges. The solubility of nickel in the spinel solid solution is limited to ca. 30 at%. The solubility of manganese in the $LiNiO_2$ based solid solution is limited ca. 20 at%. In the intermediate compositional range centered at around the Li:Ni:Mn=1:2:1, there exists a solid solution with structures based on the NaCl-type one. At 700°C, samples with vacancy ordered $MgNi_6O_8$-type structure [12] were obtained. At 850°C, samples with short-range ordered structure are obtained. The details of these phases will be published elsewhere.

$Li_2NiMn_3O_8$ is located at the phase boundary of $LiMn_2O_4$ based spinel solid solution obtained at 700°C. As for the Li_2NiMnO_4, the single-phase samples could not be obtained by the direct reaction of three starting materials containing Li, Ni, and Mn. They always contained some impurity phases both at 700 and 850°C. The phase relations of Li_2NiMnO_4 in the quaternary Li-Ni-Mn-O system are still uncertain even when the mixed hydroxide of Ni and Mn was employed as a starting material.

3.2 $Li_2NiMn_3O_8$ with 5V class cell operation voltage

Two samples of battery-active $Li_2NiMn_3O_8$ prepared by using nickel-manganese mixed hydroxide as a starting material were examined by TEM. The mixture together with $LiOH{\cdot}\ H_2O$ was heated at 1000°C in air for 10 hours (Sample A). After the calcination at 1000°C, samples were annealed at 700°C for 48 hours (Sample B). The $Li/Li_2NiMn_3O_8$ cell using the sample B annealed at 700°C shows flat charge-discharge curves with the operation voltage of 4.7 V. However, sample A calcined at 1000°C gives a stepwise change in the operation voltage in the charge-discharge curves. Electron microscopy observations revealed clear differences in these two samples.

Figure 2 shows electron diffraction patterns (EDPs) of above two samples. The EDPs of sample A can be indexed as a simple spinel-type structure. On the contrary, EDPs of sample B annealed at 700°C show weak but sharp extra-spots at the reciprocal lattice points forbidden for the spinel-type structure. No extra spots indicating the multiplicity of the unit cell was not observed. It is to be noted that 200 spots in the [100]-zone diffraction patterns are very weak. This suggests some extinction condition for the diffraction spots. In the case of EDPs of spinel structure, double diffraction effect is prominent. As can be clearly seen in the [110]-zone diffraction patterns, forbidden 200 spots show fairly strong intensity. The close examination of powder x-ray diffraction patterns of sample annealed at 700°C indicated that the extinction condition of 00ℓ: $\ell \neq 4n$ (n: integer), which agrees with the $P4_332$ or $P4_132$ space group symmetry of the 1:3 ordered structure in the spinel B sites reported for $Li_2NiMn_3O_8$ [13], $LiFe_5O_8$[14], and $LiAl_5O_8$ [15].

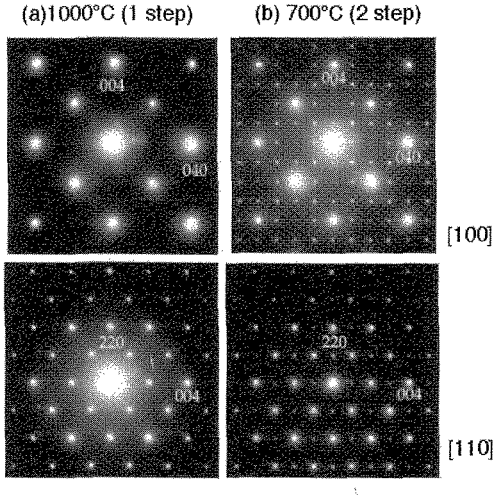

Fig. 2 Electron diffraction patterns of $Li_2NiMn_3O_8$ prepared by heating $(Ni_{0.5}Mn_{0.5})(OH)_2$ and $LiOH{\cdot}H_2O$ at1000°C (a) and then annealed at 700°C (b)

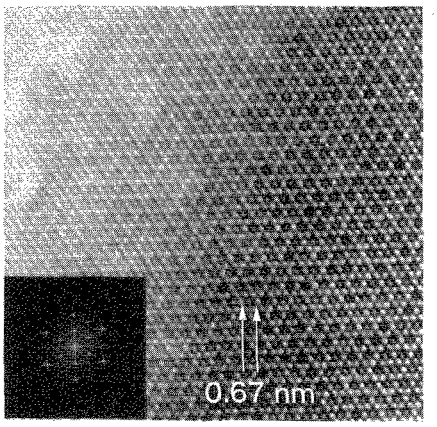

Fig.3 A lattice image of $Li_2NiMn_3O_8$ annealed at 700°C viewed along [111]

Figure 3 shows a lattice image of the sample annealed at 700°C viewed along the [111] direction. Lattice fringes with the spacing (6.7Å) twice the (220) lattice spacing are clearly seen along the three equivalent directions. The weaker contrast of this lattice fringes in the thinner region near the crystal edge is ascribable to the small difference in the atomic scattering factors of Ni and Mn. Because no effect of double diffraction occurs in this zone axis, the lattice image in Fig. 3 indicates that the 1:3 ordering of Ni and Mn is nearly perfect.

The necessity of the low temperature annealing to obtain the sample with good cell performance can be suggested from the composition-product diagram shown in Fig. 1. When samples were annealed at 850°C in air, $Li_2NiMn_3O_8$ is not a stable phase and it decompose into a spinel phase with lower Ni content and a NaCl-type solid solution with SRO arrangement of cations. In fact, a few particles showing ED pattern of $MnNi_6O_8$-type ordering were observed in the samples calcined only at 1000°C. The TG-DTA measurements indicate that 700°C is the upper limit of the stability of $Li_2NiMn_3O_8$.

3.3 Li_2NiMnO_4 with high rechargeable capacity ca. 200mAh/g

The single-phase and cell-active samples of Li_2NiMnO_4 were obtained by heating the stoichiometric mixture of $LiOH{\cdot}H_2O$ and $(Ni_{0.5}Mn_{0.5})(OH)_2$ at 1000°C for 15h in Air. Their powder x-ray diffraction patterns could be indexed by assuming the space group $R\bar{3}m$ of a-$NaFeO_2$-type structure (a=2.893Å and c=14.31Å). However, the Rietveld profile analysis based on the $R\bar{3}m$ space group leads to a site exchange of about 10% between Li and transition metals [11].

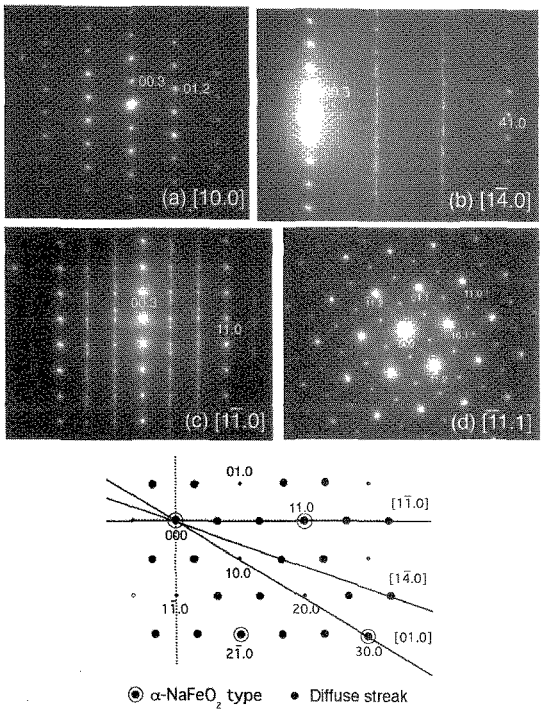

Fig. 4 ED patterns of Li_2NiMnO_4; (a) [10.0], (b)[1$\bar{4}$.1], (c) [$\bar{1}$1.0], (d) [$\bar{1}$1.1] zone of R3m lattice in hexagonal setting, (e) The positions of the diffuse streaks projected on (00.1)* reciprocal lattice plane

Figures 4(a)-(d) show EDPs observed with several different beam incidences. An EDP in Fig. 4(a) can be indexed as the [10.0]-zone EDP of α-$NaFeO_2$-type structure and shows no extra spots. Therefore, the basic structure is composed of cubic ABCABC stacking of oxygen close packed layer or tri-angular 2D lattice of octahedrally coordinated cations (so-called O3 structure). A high-resolution lattice image in Fig. 5 viewed along the [10.0] direction clearly reveals the cubic stacking. However, when the crystal was rotated around the [00.1] axis, extra diffuse streaks parallel to the reciprocal 00.L* raw were observed as shown in Fig. 4(b) and (c). From the several EDPs obtained by rotating the sample around [00.1] axis, the positions of the diffuse streaks projected on the (00.1)* reciprocal plane was deduced as shown in Fig. 4(e). A $\sqrt{3}\times\sqrt{3}$ superlattice in the transition metal or Li layers of α-$NaFeO_2$-type structure is indicated form their positions. The [$\bar{1}$ 1 .1] zone diffraction pattern in Fig. 4(e) also shows extra spots indicating the in-plane $\sqrt{3}\times\sqrt{3}$ superlattice.

The diffuse streak means that the stacking of the $\sqrt{3}\times\sqrt{3}$ ordered layer is disordered. The lattice image shown in Fig. 6 revealed many stacking faults in a crystal. However, the diffuse streak accompanies several spotty intensity maxima. Although their positions and intensity are different from place to place even in a single particle, it is suggested that the $\sqrt{3}\times\sqrt{3}$ ordered layer are stacked with some inter-layer correlations. From the positions of spotty intensity maxima, a tentative monoclinic supelattice with C2/m space group symmetry could be deduced. The lattice parameters of the monoclinic cell fulfill the following relations to the hexagonal cell parameters, a_h and c_h, of α-$NaFeO_2$-type structure; $a_m=\sqrt{3}a_h$, $b_m=3a_h$, $c_m\sin\beta=c_h/3$, $c_m\cos\beta=a_h/\sqrt{3}$.

Figure 7 shows a lattice image viewed along the [001] direction of the monoclinic supercell, which is equivalent to the [$\bar{1}$ 1 .1] direction of hexagonal cell. The lattice image reveals a region showing pseudo-hexagonal white dots array with the spacing of 4Å nearly equal to $\sqrt{3}a_h$. However, there size is limited to several nano-meters in diameter. In plane $\sqrt{3}\times\sqrt{3}$ order seems to be short-ranged although it is obscured by the stacking faults.

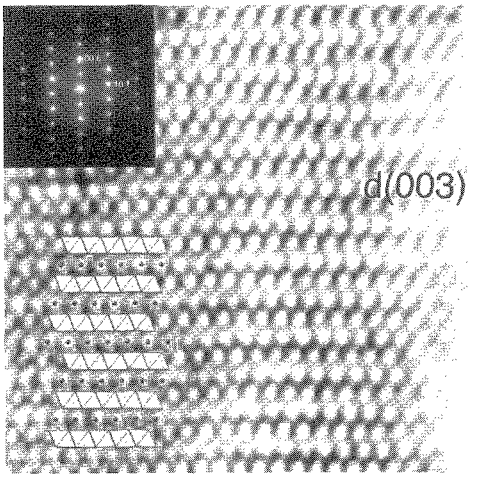

Fig.5 A lattice image of Li_2NiMnO_4 viewed along the [10.0] referring to R3m lattice

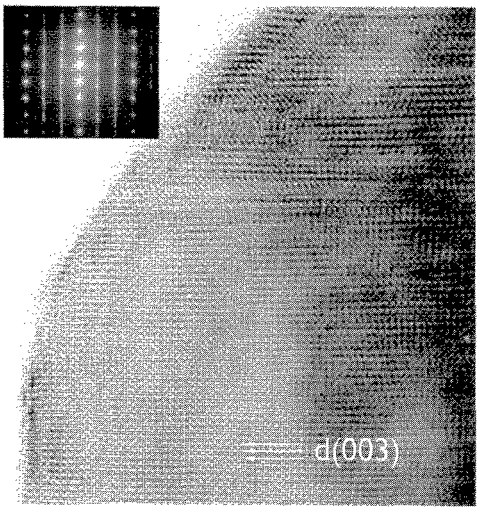

Fig.6 A lattice image of Li_2NiMnO_4 viewed along the $[\bar{1}1\ .0]_{R3m}$ indicating stacking disorder

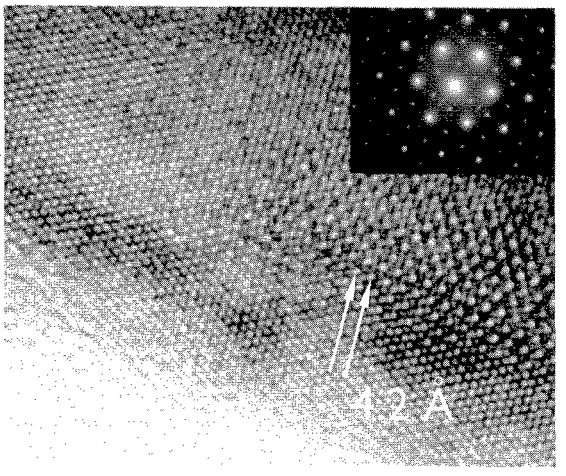

Fig. 7 A lattice image of Li_2NiMnO_4 viewed along the $[\bar{1}1\ .1]_{R3m}$ indicating in-plane short-range ordering

The powder x-ray diffraction patterns of Li_2NiMnO_4 also show traces of the short range ordering and the stacking faults observed by TEM. Very weak and broad peaks with d-spacings of 4.34 and 4.14Å are always observed. These d-values correspond to the (020) and ($\bar{1}$ 1 0) lattice spacing of C2/m monoclinic cell.

The origin of observed $\sqrt{3}\times\sqrt{3}$ in-plane cationic short range ordering or compositional modulation is uncertain at the present stage. The layer stacking in a monoclinic C2/m symmetry reminds us the structure of Li_2MnO_3 with alternate stacking of $\sqrt{3}\times\sqrt{3}$ ordered $LiMn_2$ layers and Li layers [16]. A model assuming the short-range $\sqrt{3}\times\sqrt{3}$ ordering of Li and transition metal caused by the inter-layer site exchange may seem to agree with the TEM observations. However, as mentioned above, 10% site exchange is necessary to reproduce the observed powder x-ray diffraction pattern. Such a large content of the transition metal in the Li layers should cause the poor cell performance as seen in the case of $LiNiO_2$. The actual charge-discharge characteristics of Li_2NiMnO_4 positive-electrode, particularly the smooth lattice expansion and contraction, do not agree with the presence of so much transition metal atoms in the Li layers. It is well known that the equi-molar AB system on the triangular lattice is strongly frustrated one in which any ordered structures are not stabilized without the second-neighbor interaction. [17] A strong preference of the second-neighbor pair formation for the same kind of metal may be an origin of $\sqrt{3}\times\sqrt{3}$ order in Li_2NiMnO_4.

4. SUMMARY

High resolution TEM observations have revealed cationic orderings in two new positive-electrode materials for rechargeable lithium ion batteries. In the case of $Li_2NiMn_3O_8$, the well-ordered arrangement of Ni and Mn leads to the good cell performance. The correlation of cationic ordering in Li_2NiMnO_4 and the cell performance is not clear at the present stage. We have also made TEM studies for several samples with the compositions deviated from the Li_2NiMnO_4 stoichiometry. Also, recently Kim et al. has reported a TEM study for $Li[Li_{0.1}Ni_{0.35}Mn_{0.55}]O_2$. [18] However, the short-range ordered nature is not so different. On the contrary, the cell performance shows some degradation as the composition deviates from the stoichiometry. Efforts to get well ordered samples and detailed TEM study are still under way.

ACKNOWLEGEMENT

Most of the TEM work was performed under the Visiting Researcher's Program of the Institute for Solid State Physics, the University of Tokyo. Thanks to Mr. M. Ichihara for the help in TEM observation.

REFERENCES

[1] J. R. Dahn, U. von Sacken, and C. A. Michal, *Solid State Ionics*, **44**, 87 (1990)
[2] T. Ohzuku, A. Ueda, and M. Nagayama, *J. Electrochem. Soc.*, **140**, 1862 (1993).
[3] Ohzuku, S. Takeda, and M. Iwanaga, *J. Power Sources*, **81-82**, 90 (1999)
[4] T. Ohzuku, A. Ueda, and M. Kouguchi, *J. Electrochem. Soc.*, **142**, 4033 (1995)
[5] T. Ohzuku, K. Ariyoshi, S. Yamamoto, and Y. Makimura, *Chem. Letters*, 1270 (2001).
[6] T. Ohzuku, K. Ariyoshi, and S. Yamamoto, *J. Ceramic Soc. Jpn.*, **110**, 501(2002).
[7] K. Ariyoshi, S. Yamamoto, and T. Ohzuku, *J. Power Sources*, 119-121, 959 (2003).
[8] K. Ariyoshi, Y. Iwakoshi, N. Nakayama and T. Ohzuku, *J. Electrochem. Soc.*, to appear
[9] T. Ohzuku and Y. Makimura, *Chem. Lett.*, 744 (2001)
[10] Y. Makimura and T. Ohzuku, *J. Power Sources*, **119-121**, 156 (2003)
[11] Y. Makimura, N. Nakayama and T. Ohzuku, *ECS meeting proceedings*, spring 2003, to appear
[12] A. Feltz and Töpfer, J. Alloys Compds., 196, 75 (1993)
[13] D. Gryffroy, R. E. Vandenberghe, and E. Legrand, *Mater. Sci. Forum*, **79-82**, 785(1991)
[14] P. Baum, *Nature* (London) 170, 1123(1952)
[15] R. Portier, S. Lefebvre and M. Fayard, Mater. Res. Bull., 10, 883 (1975)
[16] P. Strobel and B. Lambert-Andron, J. Solid State Chem., 75, 90 (1988)
[17] M. Schick, J. S. Walker and M. Wortis, Phys. Rev. B16, 2205 (1977)
[18] J. H. Kim, C. S. Yoon, and Y. K. Sun, J. E, *J. Electrochem. Soc.*, **150**, 538 (2003).

(Received October 13, 2003; Accepted December 14, 2003)